Trapped Surfaces in 2+1 Dimensions

Emma Jakobsson

Master's Thesis in Theoretical Physics

Department of Physics
Stockholm University
Stockholm, Sweden 2011

Department of Physics

Abstract

Trapped surfaces are the precursors of singularities in gravitational collapse. In numerical simulations it has been found that trapped surfaces can make sudden "jumps" from one location to another. When a lump of matter hits a trapped surface it is believed that the trapped surface moves outwards. This behaviour is difficult to describe analytically in a 3+1-dimensional spacetime because gravitational radiation is emitted. In this master's thesis the problem is tackled in 2+1 dimensions where things become simpler. By considering a toy model of a black hole in 2+1-dimensional anti-de Sitter space, and letting a point particle fall into the black hole, an exact description of this peculiar behaviour of the trapped surfaces is found.

Fångade ytor i 2+1 dimensioner

Fångade ytor förebådar singulariteter i gravitationskollaps. I numeriska simulationer har det observerats hur fångade ytor kan göra plötsliga "hopp" från en plats till en annan. När en fångad yta träffas av en klump materia tros den fångade ytan flytta sig utåt. Detta beteende är svårt att beskriva analytiskt i en 3+1-dimensionell rumtid eftersom det hela kompliceras av gravitationsstrålning. I detta masterarbete närmas problemet därför i 2+1 dimensioner, vilket förenklar saken. Genom att betrakta en leksaksmodell av ett svart hål i 2+1-dimensionella anti-de Sitterrummet, och låta en punktpartikel falla in i detta svarta hål, hittas en exakt beskrivning av detta lustiga beteende hos de fångade ytorna.

Acknowledgements

I would like to thank my supervisor Ingemar Bengtsson for his enthusiastic and invaluable guidance, and for being a great source of inspiration. I would also like to thank Sören Holst for the figures 2.4, 2.5 and 4.2 which were greatly inspired by originals made by him for his PhD thesis *Horizons and Time Machines - Global Structures in Locally Trivial Spacetimes* [6]. Also figure 4.3 was originally drawn by Dieter Brill.

Contents

Chapter 1

Introduction

The existence of a black hole in a 2+1-dimensional spacetime with constant negative curvature was first discovered by Bañados *et al* [1]. We call this a BTZ black hole. In this thesis we look at such a black hole in 2+1-dimensional anti-de Sitter space. It is a *toy model* of a real black hole which of course exists in a four dimensional spacetime. The point of removing one spatial dimension is to greatly simplify matters, but with the hope of being able to illustrate something that can be useful in the full 3+1-dimensional spacetime. The goal of this thesis is to study the behaviour of *trapped surfaces* which are the precursors of singularities in gravitational collapse.

A trapped surface is defined as a closed spacelike surface such that both families of light rays orthogonal to it converge. Since there must be two null directions orthogonal to it, the dimension of the surface is two less than the spacetime it lies in. In a 2+1-dimensional spacetime the trapped surfaces therefore become one dimensional, so they appear as trapped *curves* rather than surfaces. The concept of trapped curves might seem unintuitive. Consider for example the closed curve of Fig. 1.1 in a flat spacetime. At each point along the curve there are two null vectors orthogonal to it, one directed inwards and one directed outwards. As we see in the picture the inwards directed family of null vectors converges, while the outwards directed family diverges. Hence the curve is not trapped. If we instead consider a curve which is the intersection of two backward light cones, by construction the curve will have the property that both families of light rays orthogonal to it converge. However the curve is not closed, so by definition it is not trapped. In fact there are no trapped curves in a flat spacetime.

Trapped surfaces appear in singular spacetimes and for that reason we

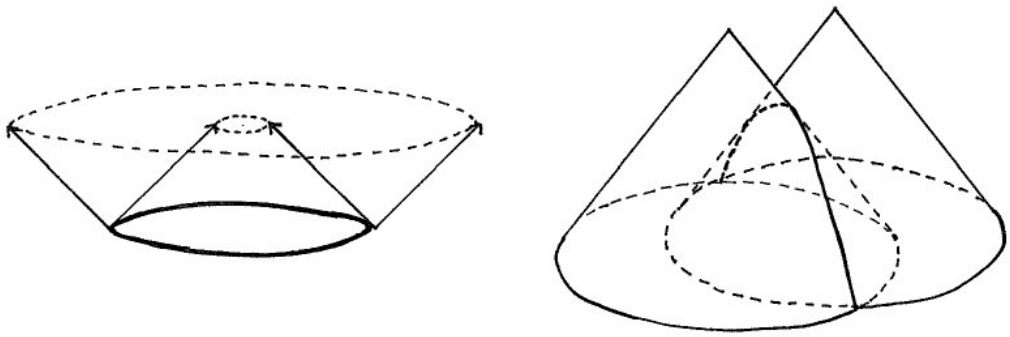

Figure 1.1: Curves in flat space. The curve to the left is closed, but one of the families of light rays orthogonal to it diverges. The curve to the right is constructed so that both families of light rays converge, but it is not closed. Neither of the curves is trapped.

turn our attention to black holes. A model of a black hole requires a singularity that is hidden behind an event horizon. The event horizon is a boundary in spacetime such that no event inside this boundary can be seen from the outside. To tell if an event could be seen from the outside at any time, one must know what spacetime looks like at *all* times. Thus the event horizon is a *global* property since its definition requires a full description of spacetime. A black hole is usually defined as the interior of this boundary. A trapped surface on the other hand is *quasilocal*; it only involves the surface itself and its infinitesimal surroundings. The hypothesis of cosmic censorship states that no naked singularities exist; they are always made invisible by an event horizon. Moreover, according to this conjecture, the event horizon lies outside the region containing trapped surfaces. Thus a trapped surface could not be observed experimentally.

Nonetheless the concept of trapped surfaces is of importance in different areas. One of them is the field of quantum gravity. A possibility is that quantum gravity modifies the spacetime in a way such that it will not contain singularities. Perhaps it is possible to send signals to the outside through the classically singular region. In that case the event horizon can not be defined. However, trapped surfaces would survive in such a theory. Even though quantum gravity might eliminate singularities, we know that there is a region of spacetime that behaves in a classical manner. A trapped surface, since it

is quasilocal, could therefore be defined in such a region. Trapped surfaces are also of interest in numerical relativity, where they are of a more practical use. Given initial data one can numerically compute how a spacetime evolves with time. Such a simulation can only cover a finite time interval, hence it is only possible to read off local or quasilocal entities. The location of the event horizon can not be found in the simulation since one must have information about the infinite future to know where it is. This is why trapped surfaces become important. With the help of effective algorithms, it is possible to tell if a spacelike hypersurface in the simulation contains a trapped surface. The presence of a trapped surface indicates that a black hole has been created. There are singularity theorems [2] that say that a singularity must occur in the future of a trapped surface for every reasonable matter model. Assuming that cosmic censorship holds, this singularity must be hidden by an event horizon. Even though the event horizon can not be seen in the simulation, the trapped surface indicates that this boundary has been crossed, since, according to the cosmic censorship hypothesis, trapped surfaces can not exist outside the event horizon. Thus the appearance of a trapped surface is the only practical way to determine if a black hole has been created.

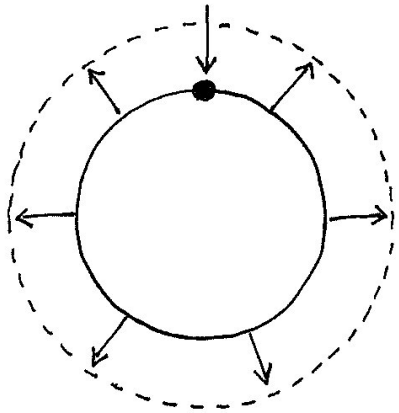

Figure 1.2: When a lump of matter hits a trapped surface, the surface moves outwards.

In these simulations the trapped surfaces have been observed to sometimes "jump" from one location to another in a rather peculiar way [3, 4]. When a lump of matter hits a trapped surface, it is believed that the trapped

surface moves outwards. Not only at the point where it was hit, but along the whole surface, see Fig. 1.2. This nonlocal behaviour explains why trapped surfaces are *quasi*local rather than local. It is difficult to find an analytic description of this behaviour in 3+1 dimensions because gravitational radiation would be emitted, making the spacetime metric hard to express in any formula. But in 2+1 dimensions, where there is no gravitational radiation [5], the problem becomes simpler. By letting a point particle fall into the 2+1-dimensional toy model of a black hole, we get an exact solution in which the trapped curves make these jumps. We then have the full picture of this behaviour, and do not have to rely on a given family of spacelike surfaces covering a finite time interval as in a simulation.

Chapter 2

Anti-de Sitter space

Anti-de Sitter space is a spacetime with constant negative curvature and it solves Einstein's equations with a negative cosmological constant λ. A nonzero cosmological constant generates an extra force between particles. This force is repulsive if $\lambda > 0$ and attractive if $\lambda < 0$. Although the cosmological constant has been observed to be positive, anti-de Sitter space is of interest for example in string theory. As we will see anti-de Sitter space also is of use when making a model of a black hole in 2+1 dimensions.

Before we get to its definition it is perhaps a good idea to first consider a simple example of a curved space. A very familiar example is the sphere, which is a two dimensional surface with constant *positive* curvature. A sphere with radius one can be defined as the surface

$$X^2 + Y^2 + Z^2 = 1 \tag{2.1}$$

embedded in a three dimensional Euclidean space coordinated by X, Y, Z. We think of this embedding in a higher dimensional space as the natural way to view the sphere. A three dimensional sphere, or a 3-sphere, with radius one is similarly defined as the *hypersurface*

$$X^2 + Y^2 + U^2 + V^2 = 1 \tag{2.2}$$

embedded in a four dimensional Euclidean space coordinated by X, Y, U, V. By adding an extra dimension we can no longer draw a picture of the sphere in the embedding space, and for that reason the three dimensional sphere might seem a bit more difficult to fully grasp.

By changing a sign in the quadric we obtain a hyperboloid rather than a sphere. For example, the two-sheeted hyperboloid

$$X^2 + Y^2 - Z^2 = -1 \tag{2.3}$$

is a two dimensional surface of constant *negative* curvature if embedded in 2+1 dimensional Minkowski space with metric

$$ds^2 = dX^2 + dY^2 - dZ^2. \tag{2.4}$$

The upper sheet of this hyperboloid is called the hyperbolic plane. It is a spacelike surface, but unlike the sphere it can not be globally embedded in a Euclidean space. Just like we defined the three dimensional sphere, higher dimensional hyperbolic spaces can easily be defined by adding extra dimensions.

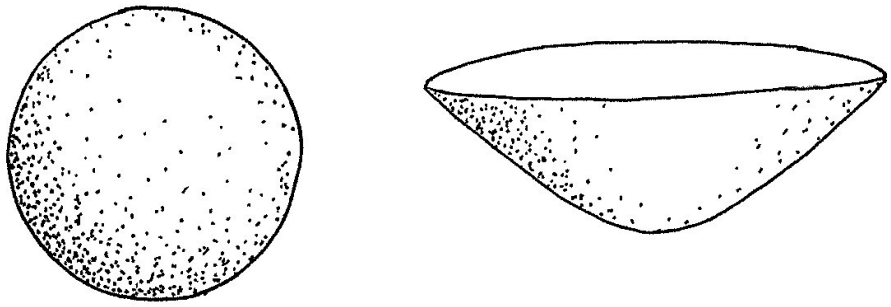

Figure 2.1: The sphere and the hyperbolic plane.

After having considered spheres and hyperboloids, it is perhaps time to get to know anti-de Sitter space. In 1+1 dimensions it is defined as the surface

$$X^2 - U^2 - V^2 = -1 \tag{2.5}$$

embedded in a flat spacetime with metric

$$ds^2 = dX^2 - dU^2 - dV^2. \tag{2.6}$$

It is easy to draw a picture of this surface in the embedding space, where it looks like the one-sheeted hyperboloid shown in Fig. 2.2. Note that the embedding space has *two* timelike dimensions, U and V. Closed curves going

around the hyperboloid will be timelike, but this is not something we need to worry about in this thesis. Defining 2+1 dimensional anti-de Sitter space is now straightforward. The defining quadric is

$$X^2 + Y^2 - U^2 - V^2 = -1, \tag{2.7}$$

where X, Y, U and V are coordinates in a flat four dimensional spacetime with metric

$$ds^2 = dX^2 + dY^2 - dU^2 - dV^2. \tag{2.8}$$

The embedding coordinates X, Y, U, V are convenient when performing calculations, but are not the best choice for visualization since we can not draw a picture of the spacetime using them. For this purpose, let us introduce the *sausage coordinates* as invented by Holst [6].

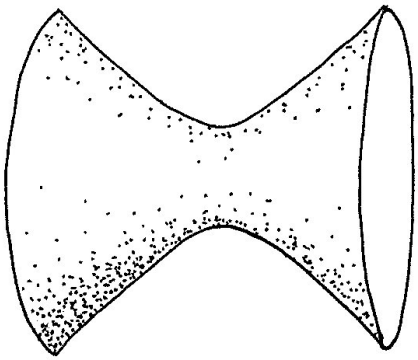

Figure 2.2: 1+1 dimensional anti-de Sitter space.

2.1 Sausage coordinates

To derive the sausage coordinates set $U = Z\cos t$, $V = Z\sin t$. When Z ranges from zero to infinity and t ranges from, say, $-\pi$ to π all of anti-de Sitter space is covered. The defining quadric becomes exactly that of Eq. (2.3) and the metric becomes

$$ds^2 = dX^2 + dY^2 - dZ^2 - Z^2 dt^2. \tag{2.9}$$

With $dt = 0$ the metric becomes that of 2+1 dimensional Minkowski space (Eq. (2.4)). So, since Z was defined to be positive, we see that surfaces of constant t are hyperbolic planes.

The next step is to map these hyperbolic planes at constant t to the XY-plane. This is done by means of stereographic projection. The idea is to draw a straight line from the point $(X, Y, Z) = (0, 0, -1)$ to a given point on the hyperboloid where $Z > 0$. The point on the hyperboloid is then projected to the point where this line intersects the XY-plane, see Fig. 2.3. Lines from the projection point $(0, 0, -1)$ intersecting the hyperboloid will all be timelike. As we approach spatial infinity on the hyperboloid these lines will come closer to being lightlike. Since lightlike lines through the projection point intersect the XY-plane along a circle with radius one we see that the whole hyperboloid is projected onto the interior of the unit disk. This is the so-called *Poincaré disk*, on which we will use polar coordinates ρ and φ.

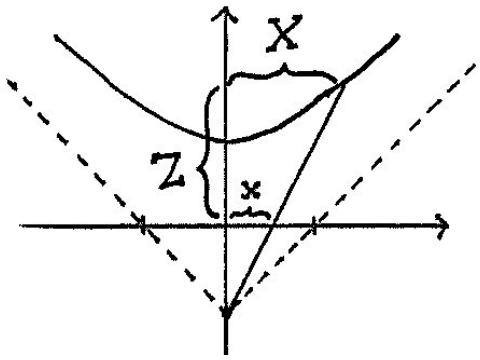

Figure 2.3: Stereographic projection of the hyperboloid in the XZ-plane. The point $(X, 0, Z)$ on the hyperboloid is projected to the point $(x, 0)$ on the Poincaré disk. In polar coordinates $x = \rho \cos \varphi$. Lightlike lines (dotted) through the projection point will not intersect the hyperboloid which is therefore projected onto the interior of the unit disk $\rho < 1$.

The explicit relation between the embedding coordinates X, Y, U, V and

the sausage coordinates t, ρ, φ is

$$\begin{aligned} X &= \frac{2\rho}{1-\rho^2}\cos\varphi, \\ Y &= \frac{2\rho}{1-\rho^2}\sin\varphi, \\ U &= \frac{1+\rho^2}{1-\rho^2}\cos t, \\ V &= \frac{1+\rho^2}{1-\rho^2}\sin t. \end{aligned} \tag{2.10}$$

The metric becomes

$$ds^2 = -\left(\frac{1+\rho^2}{1-\rho^2}\right)^2 dt^2 + \frac{4}{(1-\rho^2)^2}(d\rho^2 + \rho^2 d\varphi^2). \tag{2.11}$$

The map that takes the hyperbolic plane to the Poincaré disk is *conformal*, meaning that it preserves angles. In fact the projection point was chosen such that this would be the case. However distances are distorted by the projection. The metric on the Poincaré disk, given as the last term of Eq. (2.11), is the flat metric multiplied by a factor. The effect of this factor is small for small values of ρ, but as ρ approaches one it becomes larger. It means that points close to the boundary $\rho = 1$ lie farther away from the origin than one might expect just by looking at the picture. At the boundary the factor in front of the metric diverges. But this can easily be helped by multiplying the metric by a conformal factor Ω. For example we could choose

$$\Omega = \frac{1-\rho^2}{1+\rho^2}, \tag{2.12}$$

and define

$$d\hat{s}^2 = \Omega^2 ds^2 = -dt^2 + \frac{4}{(1+\rho^2)^2}(d\rho^2 + \rho^2 d\varphi^2). \tag{2.13}$$

Even though this new metric does not give correct distances, it has the advantage that it is well behaved on the boundary $\rho = 1$. The boundary is referred to as *conformal infinity* [2], or $\mathcal{J}$ (pronounced "scri"). Through the projection of space onto the Poincaré disk, space has been *conformally compactified*, since it is possible to bring infinity to a finite distance from the origin through a conformal rescaling.

Another example of a conformal compactification is the *Riemann sphere* known from complex analysis. It is obtained by mapping the complex plane to a unit sphere using stereographic projection. If the position of the sphere is chosen such that the complex plane lies in the equatorial plane of the sphere, or in a plane parallel to it, and the projection point is chosen to be the south pole, then conformal infinity will be at the north pole; it is just a point. A conformal compactification of the hyperbolic plane on the other hand can not yield a conformal boundary that is just a point, it must be a circle. The reason for this is that in some sense there is "more space" close to infinity in the hyperbolic plane than in the flat plane.

Getting back to anti-de Sitter space, we can now draw a compact picture of it as a pile of Poincaré disks, where each disk corresponds to a surface of constant coordinate time t, see Fig. 2.4. This cylinder might remind of a salami, whose slices consist of Poincaré disks, hence the name of the coordinates.

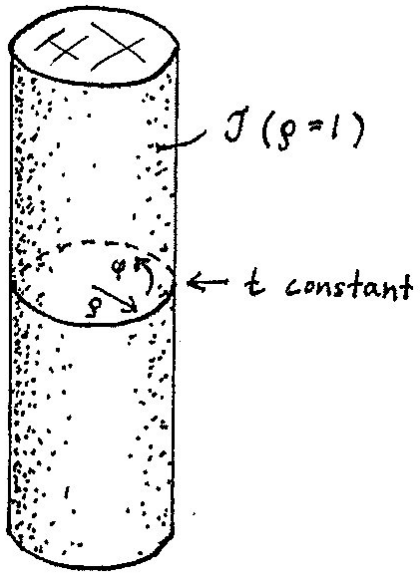

Figure 2.4: Anti-de Sitter space in sausage coordinates. A surface of constant t is a Poincaré disk coordinated by ρ and φ. The surface of the cylinder at $\rho = 1$ represents conformal infinity $\mathcal{J}$.

Regarding the nature of $\mathcal{J}$ it is worth noting that it is timelike. In fact it

can be shown that any spacetime that can be conformally compactified will have a timelike $\mathcal{J}$ if the cosmological constant λ is negative, while $\mathcal{J}$ will be spacelike if $\lambda > 0$ and lightlike if $\lambda = 0$ [2]. This is something that we will get back to, since it will turn out that the nature of $\mathcal{J}$ is of importance when making a model of a black hole.

2.2 Geodesics

Let us now turn to the analogue of a straight line in a curved space, or a *geodesic*. In a Euclidean space most of us think it is obvious what is meant by a straight line, even though we may not know how to define it. If one thinks about it a straight line between two points can be defined as the shortest path between these two points. This also holds in a curved space. For example, there are no straight lines on a sphere since the surface of the sphere is curved. But we can define a geodesic on the sphere to be a curve such that it follows the shortest path between two points on the curve, as long as these points are not too far apart. The vague condition that the distance between the points is small enough is not needed in a more careful definition of a geodesic. A geodesic is always given as the solution of a differential equation, see for example Schutz [7]. Given initial values, i.e. a point and a direction, a geodesic will then be uniquely determined.

Geodesic paths on the sphere are great circles. A great circle on a 2-sphere centered at the origin is obtained as the intersection of the sphere and a plane containing the origin. On a 3-sphere such an intersection, an "equator", is in itself a two dimensional surface; in fact it is a 2-sphere. Geodesic paths on this surface, i.e. great circles, are also geodesic paths on the 3-sphere. This property makes the equator a *totally geodesic surface*. Also in anti-de Sitter space the intersection of a hyperplane containing the origin and the hypersurface $X^2 + Y^2 - U^2 - V^2 = -1$ is a totally geodesic surface, meaning that geodesics on such a surface are also geodesics in anti-de Sitter space. The equation of a hyperplane containing the origin in the embedding space is

$$\boldsymbol{a} \cdot \boldsymbol{X} = 0, \tag{2.14}$$

where $\boldsymbol{a} = (a_1, a_2, a_3, a_4)$ is the normal vector to the hyperplane and $\boldsymbol{X} = (X, Y, U, V)$ is a vector in the embedding space. An expression of a totally geodesic surface in sausage coordinates is found using Eqs. (2.10) and (2.14). This surface, which is a plane in the embedding space, will be timelike if

$\boldsymbol{a}^2 > 0$, lightlike if $\boldsymbol{a}^2 = 0$ and spacelike if $\boldsymbol{a}^2 < 0$. Set

$$\boldsymbol{a} = (a\sin\alpha, a\cos\alpha, b\sin\beta, b\cos\beta), \tag{2.15}$$

where a, b, α and β are arbitrary constants, and we find that the two dimensional plane containing geodesics is given by

$$\frac{2\rho}{1+\rho^2}\sin(\varphi+\alpha) = \frac{b}{a}\sin(t+\beta). \tag{2.16}$$

Note that the ratio between a and b determines whether this plane is timelike, spacelike or lightlike.

To find an expression of geodesics in planes of constant φ we simply let φ be a constant in Eq. (2.16). With $\varphi + \alpha = \pi/2$ we find that the geodesic is given by

$$\frac{2\rho}{1+\rho^2} = \xi\sin(t+\beta), \tag{2.17}$$

where $\xi = b/a$. It is timelike if $|\xi| < 1$, lightlike if $|\xi| = 1$ and spacelike if $|\xi| > 1$. Some examples with $\beta = 0$ are illustrated on the left hand side of Fig. 2.5.

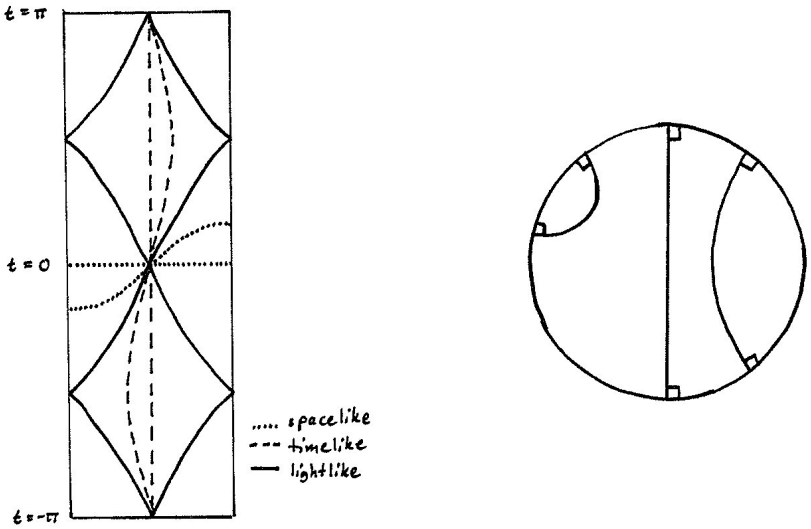

Figure 2.5: To the left geodesics in the ρt-plane in sausage coordinates. To the right geodesics on the Poincaré disk.

Let us also see what geodesics on the Poincaré disk look like. Letting t be a constant, suitably chosen to be $t = \pi/2 - \beta$, in Eq. (2.16) we find

$$\frac{2\rho}{1+\rho^2}\sin(\varphi + \alpha) = \xi, \tag{2.18}$$

where in this case the absolute value of ξ must be less than one. The geodesics described by Eq. (2.18) are arcs of circles on the Poincaré disk, which intersect the boundary of the disk at right angles, see the right hand side of Fig. 2.5.

While a pair of points on the sphere can always be connected by a geodesic, there are pairs of points in anti-de Sitter space that can not. This is not something we will dwell more on, but it is perhaps an interesting remark.

2.3 Stereographic coordinates

Apart from embedding coordinates and sausage coordinates there are many other choices of coordinates. In this section we consider *stereographic coordinates*, which will be used in section 4. While sausage coordinates are good for visualization, stereographic coordinates have the advantage that light cones look like light cones.

Instead of making a stereographic projection of *space*, as in the previous section, let us make a stereographic projection of the whole *spacetime*. We choose to make the projection to the hyperplane $U = 0$, on which we use the stereographic coordinates x, y, v. Choosing the projection point to be $(X, Y, U, V) = (0, 0, -1, 0)$ means that we only cover the part of anti-de Sitter space where $U > -1$. Following the same procedure as in the previous section we find

$$X = \frac{2x}{1-s^2}, \quad Y = \frac{2y}{1-s^2}, \quad U = \frac{1+s^2}{1-s^2}, \quad V = \frac{2v}{1-s^2}, \tag{2.19}$$

where $s^2 \equiv x^2 + y^2 - v^2 < 1$. The part of anti-de Sitter space that is covered by the projection is now represented as the interior of the one-sheeted hyperboloid $s^2 = 1$, see Fig. 2.6. The metric becomes

$$ds^2 = \frac{4}{(1-s^2)^2}(dx^2 + dy^2 - dv^2). \tag{2.20}$$

Since this metric is conformally related to the Minkowski metric, in these coordinates light cones will look just like light cones in Minkowski space.

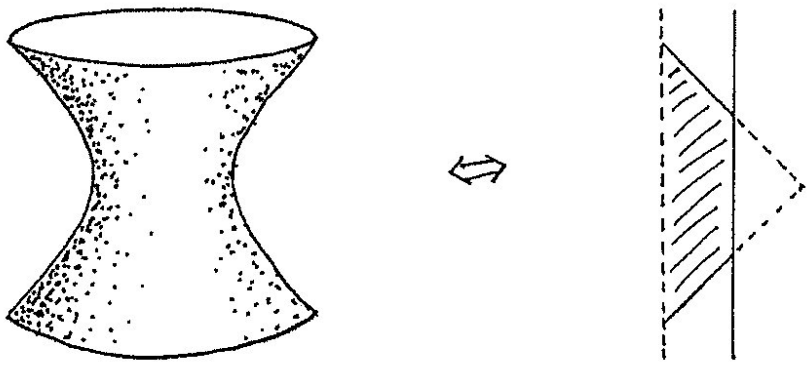

Figure 2.6: To the left is anti-de Sitter space in stereographic coordinates, represented as the interior of a one-sheeted hyperboloid. To the right is the corresponding Penrose diagram, where the shaded region shows the part of anti-de Sitter space covered by the projection.

2.4 Penrose diagrams

In section 2.1 where the sausage coordinates were derived, space was mapped onto the Poincaré disk. This led to a conformally compactified picture of anti-de Sitter space, since we saw that infinity could be brought to a finite distance by multiplying the metric by a conformal factor. The idea of this section is to do something similar, but instead of a compact three dimensional picture, we look for a compact *two* dimensional picture, a so called *Penrose diagram*. It is possible to draw a two dimensional diagram of a higher dimensional spacetime if each point in the diagram represents an orbit under a symmetry transformation. For example, an orbit under a rotation is a circle in 2+1 dimensions and a sphere in 3+1 dimensions. Both a 2+1-dimensional and a 3+1-dimensional spacetime with rotational symmetry can be represented by a two dimensional diagram if a point in this diagram represents a circle in the first case, or a sphere in the second case. The task is to find a conformal map that takes the spacetime into a finite region of 1+1-dimensional Minkowski space; even though it might not be easy to do this, there always exists such a map of any two dimensional spacetime. Light rays will then be depicted as lines with constant slope, conveniently chosen to be 45°. The result is a compact picture of the considered spacetime that captures its essential

properties.

While we are at it, it might be a good idea to draw a Penrose diagram of 2+1 dimensional Minkowski space before we get to anti-de Sitter space. It might come to use later. Letting x, y, t be the coordinates of the spacetime, we switch to polar coordinates in the xy-plane so that

$$\begin{aligned} x &= r\cos\theta \\ y &= r\sin\theta \end{aligned} \tag{2.21}$$

where r and θ has the usual range $0 \leq r < \infty$, $0 \leq \theta < 2\pi$. Light rays at constant θ are given by $t \pm r =$ constant. Now we introduce coordinates T and R such that

$$\begin{aligned} T + R &= 2\arctan(t + r), \\ T - R &= 2\arctan(t - r). \end{aligned} \tag{2.22}$$

Light rays in these coordinates will then be given by constant $T \pm R$, which are lines with 45° slope as desired. Also, this map brings infinity to a finite coordinate distance from the origin. The range of the coordinates is $-\pi \leq T \leq \pi$, $0 \leq R \leq \pi$. By letting a point (T, R) represent a whole circle at constant t and r in Minkowski space, we have obtained the desired Penrose diagram, see Fig. 2.7(a). Past and future infinity are represented by the lines $R - T = \pi$ and $R + T = \pi$ respectively. These lines are lightlike as expected in a flat space.

Now we want to draw a Penrose diagram of anti-de Sitter space. After having derived the sausage coordinates this is actually not very difficult. In section 2.2 we saw that a lightlike geodesic in a plane of constant φ was given by Eq. (2.17) with $\xi = \pm 1$. These are not straight lines with a 45° slope, but introducing a coordinate r, with range $0 \leq r \leq \pi/2$, such that

$$\frac{2\rho}{1 + \rho^2} = \sin r \tag{2.23}$$

we find that lightlike geodesics are given by $t \pm r =$ constant. With t and r as coordinates we now have our Penrose diagram of anti-de Sitter space; it is shown in Fig. 2.7(b). Infinity is represented by the timelike line $r = \pi/2$. Since the timelike coordinate t has a periodic nature, with the chosen range of t we need to identify the lines $t = \pm\pi$. Alternatively we could draw the Penrose diagram as an infinitely long strip instead of performing the identification. If we do so we will no longer have to worry about closed timelike curves.

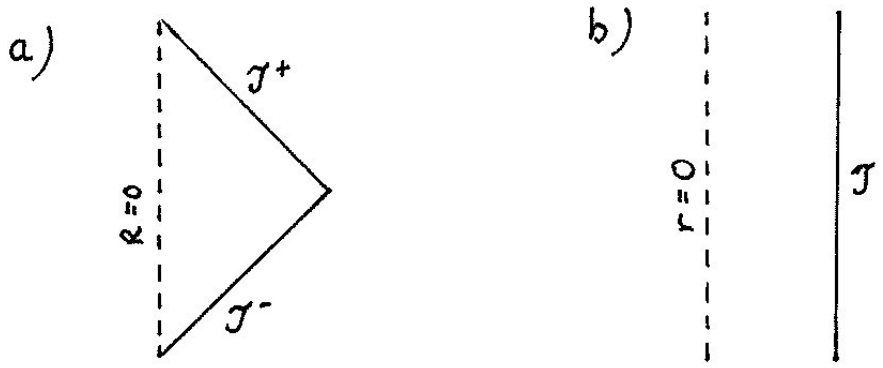

Figure 2.7: (a) Penrose diagram of Minkowski space. $\mathcal{J}^-$ and $\mathcal{J}^+$ represents past and future infinity. (b) Penrose diagram of anti-de Sitter space. In the flat Minkowski space $\mathcal{J}$ is lightlike, while it is timelike in anti-de Sitter space.

2.5 The group $SL(2,\mathbb{R})$

$SL(2,\mathbb{R})$ is the group of all two by two matrices with real matrix elements and determinant one. We can write an arbitrary group element $\boldsymbol{g} \in SL(2,\mathbb{R}))$ as

$$\boldsymbol{g} = \begin{pmatrix} U+Y & X+V \\ X-V & U-Y \end{pmatrix}, \tag{2.24}$$

if

$$\det \boldsymbol{g} = -X^2 - Y^2 + U^2 + V^2 = 1. \tag{2.25}$$

Thus we see that the group manifold of $SL(2,\mathbb{R})$ actually is anti-de Sitter space. As a comparison it might be familiar that the three dimensional sphere is the group manifold of $SU(2)$. Also the group $SU(2)$ is locally isomorphic to the rotation group $SO(3)$; the group manifold of $SO(3)$ is the 3 -sphere with antipodal points identified. Similarly there is a local isomorphism between the group $SL(2,\mathbb{R})$ and the Lorentz group $SO(1,2)$. This statement will be justified in section 3.1.

Later, when we will want to perform transformations in anti-de Sitter space, the practical way to do this will be to use $SL(2,\mathbb{R})$-matrices. Just like any group, the group $SL(2,\mathbb{R})$ can act on itself in three different ways. These are left action $\boldsymbol{g} \to \boldsymbol{g}_1\boldsymbol{g}$, right action $\boldsymbol{g} \to \boldsymbol{g}\boldsymbol{g}_1^{-1}$ and conjugation $\boldsymbol{g} \to \boldsymbol{g}_1\boldsymbol{g}\boldsymbol{g}_1^{-1}$.

There is then a group of transformations in anti-de Sitter space,

$$\boldsymbol{g} \to \boldsymbol{g}_L \boldsymbol{g} \boldsymbol{g}_R^{-1}, \tag{2.26}$$

and it is quite large since the group elements $\boldsymbol{g}_L$ and $\boldsymbol{g}_R$ of $SL(2,\mathbb{R})$ can be chosen independently. This is the group $SL(2,\mathbb{R}) \times SL(2,\mathbb{R})$, and it has just been shown that it is locally isomorphic to the anti-de Sitter group $SO(2,2)$. The group has six parameters, so it is of the same size as the Poincaré group in 2+1 dimensions. The Poincaré group is the group of isometries of Minkowski spacetime, and it can be divided into Lorentz transformations and translations in space and time.

Two group elements $\boldsymbol{g}_1$ and $\boldsymbol{g}_2$ are said to belong to the same *conjugacy class* if there is a $\boldsymbol{g} \in SL(2,\mathbb{R})$ such that $\boldsymbol{g}_2 = \boldsymbol{g}\boldsymbol{g}_1\boldsymbol{g}^{-1}$. Group elements belonging to the same conjugacy class give rise to transformations with qualitatively similar properties. For example, when dividing $SU(2)$ into conjugacy classes it turns out that elements belonging to the same conjugacy class all describe rotations through the same angle; this is Euler's theorem. Note that $\mathrm{Tr}\boldsymbol{g}\boldsymbol{g}_1\boldsymbol{g}^{-1} = \mathrm{Tr}\boldsymbol{g}_1\boldsymbol{g}^{-1}\boldsymbol{g} = \mathrm{Tr}\boldsymbol{g}_1$, so elements belonging to the same conjugacy class all have the same trace. The fact that conjugacy classes are labelled by the trace is something that will be of use later on.

Chapter 3

Point particles and singularities

Now that we are familiar with empty anti-de Sitter space, let us introduce matter. To avoid complicating the toy model more than necessary, we choose matter in the form of a point particle. A simple way to do this is by *cutting and gluing*. We begin with looking at an example in flat Minkowski space to illustrate the procedure.

3.1 Point particle in flat space

The idea is to modify our space by identifying points in it. The identification is performed using an isometry, that is a map that leaves the geodesic distance between two arbitrary points invariant. In other words the metric is left unchanged by the isometry. An example of an isometry in Minkowski space is a rotation. Consider two vertical planes intersecting along the t-axis. One of these planes can be mapped onto the other under a rotation that leaves the t-axis fixed. A wedge of spacetime is cut out by considering points that are mapped into each other identical.

The effect is that a spacelike surface at constant t now looks like a cone, as if we would have cut out a wedge of a flat piece of paper and glued the sides together, see Fig. 3.1. On the cone space is still flat everywhere except at the tip. This is where the point particle is. It can be seen as the limit of a case where a small distribution of mass curves space in a small region. We would then have a space that looks almost like a cone, but with a smooth tip. If this small mass distribution is limited to one point we get a conical singularity, assuming that we are in a two dimensional space. By the way,

in three dimensional space the same method have been used to describe infinitely long *cosmic strings*.

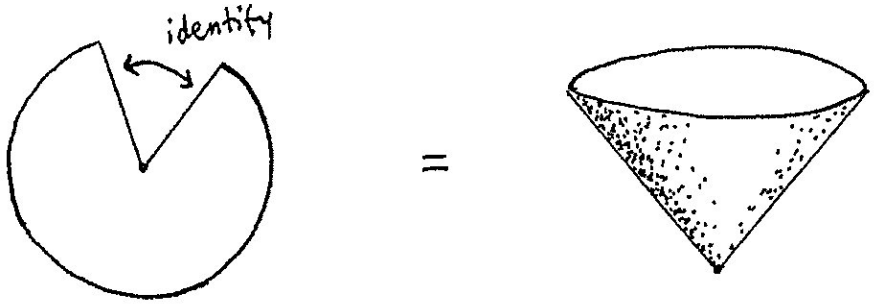

Figure 3.1: A wedge is cut out from flat space through identifying points. The result is a cone on which space is locally flat everywhere except at the tip where there is a conical singularity.

An observer in the spacetime with the point particle, not crossing the path of the particle, would not know about the particle's existence unless he travelled around it. Then he would find himself being back at the same point after turning an angle less than 2π. To be more precise, if a vector is parallel-transported along a closed curve around the conical singularity, this will cause the vector to be rotated. The angle it will be rotated by is exactly the same angle as that given by the rotation we used to perform the identification. This is called the *holonomy* of the particle.

The particle just constructed is one at rest, since its world line lies along the t-axis. But we could choose to identify points using any Lorentz transformation and the line of fixed points of this transformation would be the world line of the particle. Let us take a closer look at how we do this using group elements of $SL(2,\mathbb{R})$.

Each vector (t,x,y) in Minkowski space can be represented by a symmetric matrix

$$\boldsymbol{x} = \begin{pmatrix} t+x & y \\ y & t-x \end{pmatrix}. \tag{3.1}$$

The length squared of the vector is the determinant of the matrix $\boldsymbol{x}$:

$$\det \boldsymbol{x} = t^2 - x^2 - y^2. \tag{3.2}$$

If $\boldsymbol{g} \in SL(2,\mathbb{R})$, we can transform this vector by letting

$$\boldsymbol{x} \to \boldsymbol{x}' = \boldsymbol{g}\boldsymbol{x}\boldsymbol{g}^{\mathrm{T}}. \tag{3.3}$$

The transpose of $\boldsymbol{g}$ on the right hand side makes sure that $\boldsymbol{x}'$ is a symmetric matrix too, representing the transformed vector. Since $\det \boldsymbol{g} = \det \boldsymbol{g}^{\mathrm{T}} = 1$ we see that

$$\det \boldsymbol{x}' = \det \boldsymbol{x}. \tag{3.4}$$

Hence the length of the vector is unchanged, which is the defining property of a Lorentz transformation. This shows the local isomorphism between $SL(2,\mathbb{R})$ and the Lorentz group $SO(1,2)$. Note though that if $\boldsymbol{g} \in SL(2,\mathbb{R})$, then $-\boldsymbol{g}$ corresponds to the same Lorentz transformation, since $\boldsymbol{x} \to \boldsymbol{g}\boldsymbol{x}\boldsymbol{g}^{\mathrm{T}} = (-\boldsymbol{g})\boldsymbol{x}(-\boldsymbol{g})^{\mathrm{T}}$.

Now comes the important question of fixed points of such a transformation. Let

$$\boldsymbol{g} = \begin{pmatrix} a & b \\ c & d \end{pmatrix} \tag{3.5}$$

be an arbitrary $SL(2,\mathbb{R})$ matrix, i.e. a, b, c and d are real and $ad - bc = 1$. The fixed points of the transformation $\boldsymbol{x} \to \boldsymbol{g}\boldsymbol{x}\boldsymbol{g}^{\mathrm{T}}$ are given by

$$(t, x, y) = \sigma(b - c, b + c, d - a). \tag{3.6}$$

This defines a straight line through the origin, where σ is the parameter and $(b - c, b + c, d - a)$ the tangent vector. The length squared of the tangent vector is

$$\begin{aligned} (b-c)^2 - (b+c)^2 - (d-a)^2 &= (2 + a + d)(2 - a - d) \\ &= (2 + \mathrm{Tr}\boldsymbol{g})(2 - \mathrm{Tr}\boldsymbol{g}), \end{aligned} \tag{3.7}$$

and we see that the trace of $\boldsymbol{g}$ determines whether the line of fixed points is timelike, lightlike or spacelike. To create a particle with mass we choose a group element $\boldsymbol{g}$ with $|\mathrm{Tr}\boldsymbol{g}| < 2$ so that the world line of the particle is timelike. For a massless particle we choose $\boldsymbol{g}$ such that $|\mathrm{Tr}\boldsymbol{g}| = 2$ and the world line will be lightlike. If we were to choose a $\boldsymbol{g}$ with $|\mathrm{Tr}\boldsymbol{g}| > 2$, the line of fixed points would be spacelike. The spacetime is then that of *Misner space* [8].

3.2 Misner space

In 1+1 dimensions Misner space is achieved by identifying points through a Lorentz boost in the xt-plane. The fixed point of this transformation is at the origin. Misner space can be generalized to 2+1 dimensions by simply adding an extra dimension. Then there is a line of fixed points along the y-axis. By tilting and rotating this picture using Lorentz transformations we could map the line of fixed points onto any spacelike line in Minkowski space. But let us stick to the frame we have.

Before we move on, let us introduce some terminology by looking at a simple example. Instead of identifying points through a Lorentz boost in Minkowski space, consider the real line on which points are identified through a translation. The real line is said to be the *covering space*. When points are identified in the covering space we obtain the *quotient space*. Now we can choose a *fundamental region* in the covering space that represents the quotient space. In this example a fundamental region is an interval between two points that can be taken into each other by the given translation. Such an interval can be chosen in an infinite number of ways, so it is clear that the choice of fundamental region is not unique. Every point on the real line can then be taken to a point in the chosen interval through the given translation, so the fundamental region contains exactly one representative of every point in the quotient space. When identifying the two end points the fundamental region turns into a circle, and this circle represents the quotient space.

Now let us get back to Misner space. To avoid the complication of closed timelike curves, we limit the covering space to the shaded region of Fig. 3.2. The quotient space is obtained by identifying points through a Lorentz boost whose flow lines are also shown in the figure. The fundamental region can be taken to be the set of points between two timelike planes intersecting along the y-axis, as long as these two planes are taken into each other by the Lorentz boost, see Fig. 3.3. A spacelike surface in there has the topology of a cylinder, it is flat and free from singularities. Except at $t = 0$ where one dimension suddenly disappears; something strange happens here. Obviously there is something singular about the line of fixed points. It might seem tempting to interpret this as the world line of a particle that moves faster than light, a so-called *tachyon*, in analogy with the point particle constructed in the previous section. But we can not do so, since a closer analysis shows that this is not a conical singularity in the usual sense [8]. Instead we have an example of a singular spacetime if we remove the singularity. This spacetime

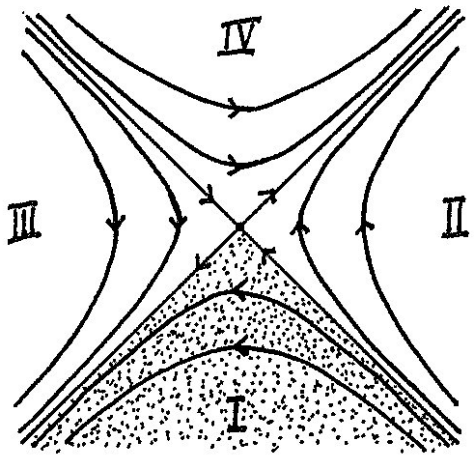

Figure 3.2: The xt-plane in Minkowski space can be divided into four quadrants bounded by lightlike lines through the origin. By taking region I (shaded) as the covering space and identifying points through a Lorentz boost, whose flow lines are shown in the figure, we obtain a singular spacetime.

is geodesically incomplete, meaning that a geodesic in there ends after only a finite parameter time when hitting the singularity. This is in fact the definition of a singular spacetime used in the singularity theorems mentioned in the introduction. However this is not a construction of a black hole. Since every lightlike particle in this spacetime will hit the singularity, there is no event horizon.

To get a full understanding of Misner space it is useful to draw a Penrose diagram. Let

$$\begin{aligned} t &= \tau \cosh \sigma \\ y &= \tau \sinh \sigma \end{aligned} \tag{3.8}$$

where $-\infty < \tau < 0$, and the range of σ is determined by the choice of identification surfaces. Lines of constant τ and x are then flow lines of the identifying transformation, and are closed to a smooth circle by the identification. Then introducing coordinates T and X such that

$$\begin{aligned} T + X &= 2 \arctan(\tau + x) \\ T - X &= 2 \arctan(\tau - x) \end{aligned} \tag{3.9}$$

does the trick. We find that $-\pi < X < \pi$, $-\pi < T < 0$ and $|X| - T < \pi$.

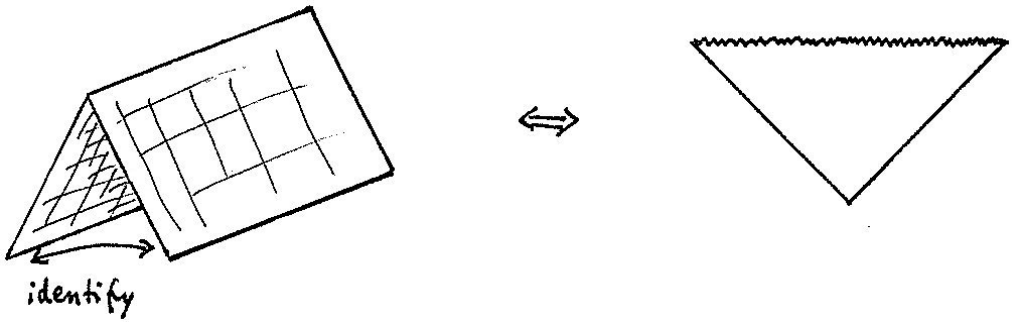

Figure 3.3: To the left is the chosen fundamental region of Misner space. To the right is the corresponding Penrose diagram.

With each point (T, X) corresponding to a whole circle, Misner space is now pictured as a triangle with the singularity at $T = 0$ and infinity represented by the lightlike lines $|X| - T = \pi$, see Fig. 3.3. With this visualization of Misner space it is obvious that every particle coming in from $\mathcal{J}$ will hit the singularity. In the Penrose diagram of Misner space we see that there are two separate asymptotic regions, two past infinities, while there was only one such in the Penrose diagram of Minkowski space that we drew in section 2.4.

3.3 Point particle in anti-de Sitter space

To create a point particle in anti-de Sitter space we use the same trick as in section 3.1. The procedure is thoroughly explained by Matschull [9]. As we saw in section 2.5 a point in anti-de Sitter space is itself represented by a group element of $SL(2, \mathbb{R})$. Transformations in anti-de Sitter space can therefore be performed by letting the group act on itself. As we already know this can be done in more than one way, but for our purposes it is enough to consider transformations that leave the unit element fixed. In other words we choose to let the group act on itself by means of conjugation.

To create a lightlike particle we choose a group element $\boldsymbol{g}_1$, with $\mathrm{Tr}\boldsymbol{g}_1 = 2$. This can for example be of the form

$$\boldsymbol{g}_1 = \begin{pmatrix} 1 & 2a \\ 0 & 1 \end{pmatrix}, \tag{3.10}$$

where a is an arbitrary real constant. Then we look for fixed points of the transformation $\boldsymbol{g} \to \boldsymbol{g}_1 \boldsymbol{g} \boldsymbol{g}_1^{-1}$, with

$$\boldsymbol{g} = \begin{pmatrix} U+Y & X+V \\ X-V & U-Y \end{pmatrix}. \tag{3.11}$$

The solution is $Y = 0$, $X = V$. In sausage coordinates this is the curve

$$\frac{2\rho}{1+\rho^2} = |\sin t| \iff \rho = |\tan(t/2)|, \tag{3.12}$$

with $\sin\varphi = 0$. Comparing this to Eq. (2.17) we see that this is a lightlike geodesic as expected. The particle will come in from infinity at time $t = -\pi/2$. Then it traverses the Poincaré disk in the ρt-plane and leaves the disk at time $t = \pi/2$, see Fig. 3.4.

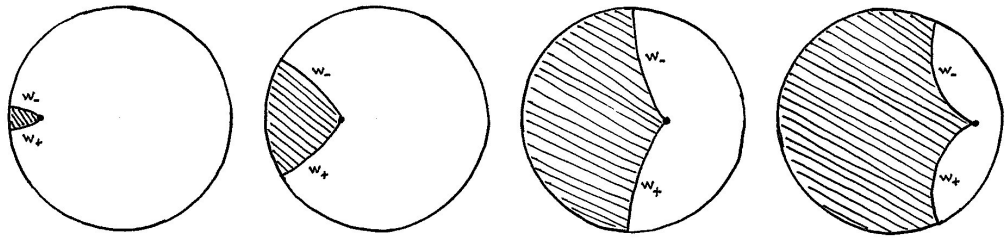

Figure 3.4: A point particle in anti-de Sitter space. The picture shows Poincaré disks at different coordinate times t. The shaded region of the disk is cut away by the identification, and the particle is at the fixed point marked by a dot. The particle enters the disk at $t = -\pi/2$ and leaves at $t = \pi/2$.

The next step is to identify points using the transformation governed by $\boldsymbol{g}_1$. We choose a fundamental region by finding two suitable identification surfaces. Since the world line of the particle is invariant under reflections in the φ-coordinate, let us see if we can find surfaces that are symmetric with respect to the plane $Y = 0$. Let the two surfaces be represented by the matrices $\boldsymbol{w}_\pm$, where $\boldsymbol{w}_-$ is transformed to $\boldsymbol{w}_+$. Now we need to solve the equation $\boldsymbol{w}_+ = \boldsymbol{g}_1 \boldsymbol{w}_- \boldsymbol{g}_1^{-1}$. With the given Ansatz we find that the surface $Y = a(V-X)$ is mapped to the surface $Y = a(X-V)$. In sausage coordinates these are given by

$$\frac{2\rho}{1+\rho^2} \sin(\varepsilon \mp \varphi) = \sin\varepsilon \sin t, \tag{3.13}$$

where a new parameter ε has been introduced, such that $\tan\varepsilon = a$. Comparing to Eq. (2.18) we see that the identification surfaces intersect surfaces of constant t along geodesics on the Poincaré disk.

Just as we did in Minkowski space we now cut out the wedge bounded by these to surfaces behind the world line of the particle. The result is a spacetime which is locally anti-de Sitter everywhere except along the world line of the particle. Again, the only way to detect the presence of the particle without crossing its world line is by travelling around it. Then one would find that the holonomy of the particle is $\boldsymbol{g}_1$.

Let us now leave this particle be for a while and instead concentrate on how to construct a black hole spacetime in anti-de Sitter space. At a later stage we will come back to the point particle when we send it into this black hole.

Chapter 4

The BTZ black hole

To construct a black hole we proceed in the same manner as before when creating a point particle. We choose a group element $\boldsymbol{g}_2$ of $SL(2,\mathbb{R})$, but this time such that $\mathrm{Tr}\boldsymbol{g}_2 > 2$. For example we could choose

$$\boldsymbol{g}_2 = \begin{pmatrix} \cosh\mu & \sinh\mu \\ \sinh\mu & \cosh\mu \end{pmatrix}, \tag{4.1}$$

with μ being an arbitrary constant, and consider the transformation $\boldsymbol{g} \to \boldsymbol{g}_2\boldsymbol{g}\boldsymbol{g}_2^{-1}$. This transformation takes the surface $Y = V\tanh\mu$ to the surface $Y = -V\tanh\mu$, and by identifying these two surfaces we can take the region of anti-de Sitter space between them to represent the quotient space. In sausage coordinates the identification surfaces are given by the equations

$$\frac{2\rho}{1+\rho^2}\sin\varphi = \pm\sin t\tanh\mu, \tag{4.2}$$

and again we see that they intersect the disks of constant t along geodesics, see Fig. 4.1. When the identification is performed the region of spacetime outside the identification surfaces is cut away. At $t = 0$ nothing is left except the singular line $Y = V = 0$ where the surfaces meet. This is where our spacetime ends.

At a first glance the result seems quite similar to Misner space. One dramatic difference though is that in Misner space $\mathcal{J}$ is lightlike, but here $\mathcal{J}$ is timelike. The difference is clearly illustrated when comparing the Penrose diagram of Misner space (Fig. 3.3) with the Penrose diagram of the BTZ black hole (Fig. 4.2). While every particle in Misner space eventually ends up at the singularity, it is possible to escape the singularity in the BTZ

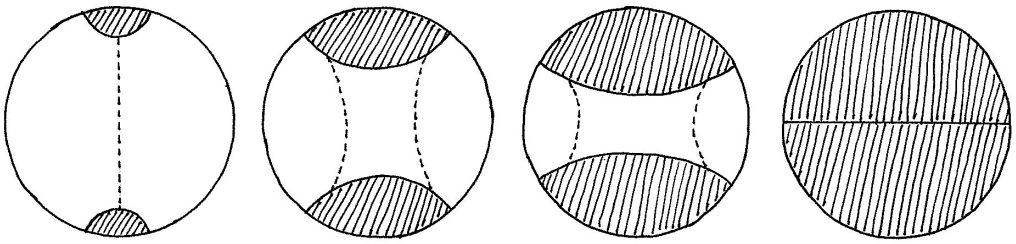

Figure 4.1: A sequence of Poincaré disks in the BTZ spacetime. The shaded regions are cut away by the identification and at $t = 0$ nothing is left but the singular line. The dotted lines show the location of the event horizon. No event between these two lines can be seen from $\mathcal{J}$.

spacetime. In other words, there exists an *event horizon*, and that is what makes this a model of a black hole.

4.1 The event horizon

The boundary of a region where every timelike or lightlike geodesic ends at the singularity is what we call the event horizon. Or, the other way around, the event horizon is the boundary of what can be seen from $\mathcal{J}$. The *last point* on $\mathcal{J}$ is the point where the singularity meets $\mathcal{J}$. Everything that can be seen from there lies on a backward light cone of this point. So the event horizon can be defined as a light cone with its vertex at the last point on $\mathcal{J}$, or a *null plane* through this point, since a null plane can be thought of as a light cone with its vertex at infinity. In the Penrose diagram of the BTZ black hole (Fig. 4.2) the event horizon is drawn as the two lightlike lines ending at the last points on $\mathcal{J}$.

Using Eq. (2.14) we find that a null plane satisfies

$$X \cos\varphi_0 + Y \sin\varphi_0 - U \cos t_0 - V \sin t_0 = 0, \tag{4.3}$$

or if we switch to sausage coordinates

$$\frac{2\rho}{1+\rho^2} \cos(\varphi - \varphi_0) = \cos(t - t_0), \tag{4.4}$$

where φ_0 and t_0 are the coordinates of the last point on $\mathcal{J}$. In our example the singularity meets $\mathcal{J}$ at the two points $(t_0, \varphi_0) = (0, 0)$ and $(t_0, \varphi_0) = (0, \pi)$.

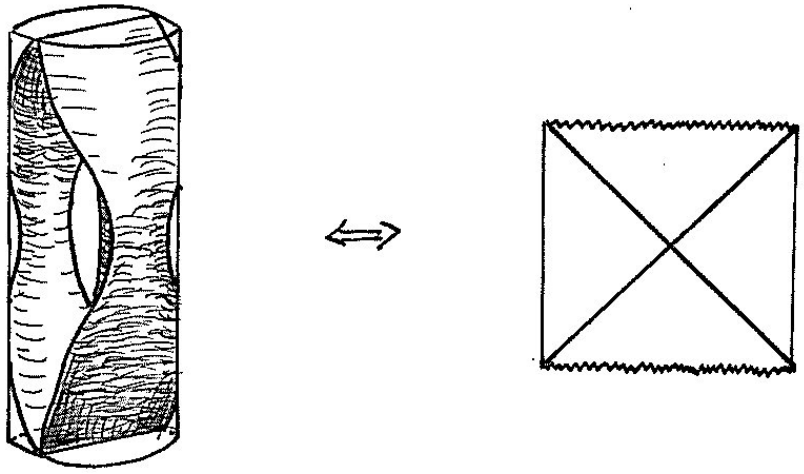

Figure 4.2: The BTZ black hole in sausage coordinates and the corresponding Penrose diagram. In the Penrose diagram we see that, just like in the Schwarzschild solution, there are two asymptotic regions.

The horizon then consists of the quotient of the two surfaces $X = \pm U$ by the isometry used to identify points. It is shown as the dotted lines of Fig. 4.1. No event between these two surfaces can be seen from $\mathcal{J}$.

But space itself does not look any different at the event horizon. A numerical relativist constructing this spacetime step by step in his computer has no chance to locate the event horizon in the simulation, unless he has knowledge about the future singularity and where it meets $\mathcal{J}$. Were he to find a *trapped curve* though, he would have a hint of what lies ahead.

4.2 Trapped curves

Consider a closed spacelike curve. Since it is spacelike there are two future directed null vectors orthogonal to its tangent vector at each point along the curve. If both these families of light rays converge, the curve is said to be *trapped*. If one family of light rays converges and the other has zero convergence, the curve is said to be *marginally* trapped. There are many different versions of trapped curves, and the terminology might be a bit confusing. Table 4.1 might make things clearer.

When dealing with trapped curves in the BTZ spacetime it is most con-

	θ_+	θ_-
Trapped	< 0	< 0
Marginally trapped	0	< 0
Outer trapped	< 0	anything
Marginally outer trapped	0	anything

Table 4.1: Different versions of trapped curves. $\theta_\pm$ are the expansions of the two families of light rays emanating from the curve.

venient to use the stereographic coordinates x, y, v, which were derived in section 2.3. The fact that these only cover the region $U > -1$ is not a problem, since we are mainly interested in the region $-\pi/2 \leq t \leq 0$ which is covered by the stereographic projection. In these coordinates the identification surfaces become the planes $y = \pm v \tanh \mu$. They intersect along the x-axis where the singularity is, see Fig. 4.3. Remembering that we are confined to the interior of the hyperboloid $x^2 + y^2 - v^2 = 1$, we conclude that the points $(x, y, v) = (\pm 1, 0, 0)$ are the last points on $\mathcal{J}$. The event horizon then consists of the two light cones with vertices at these points.

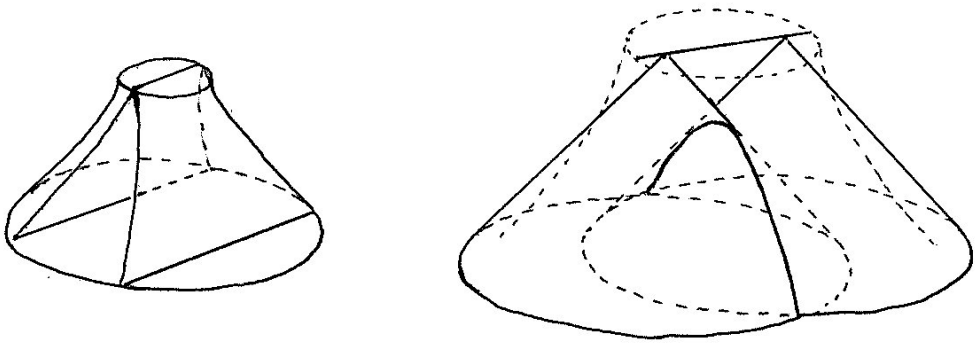

Figure 4.3: To the left is the BTZ spacetime in stereographic coordinates. Anti-de Sitter space becomes the interior of a one-sheeted hyperboloid in which the identification surfaces are drawn. To the right is the picture of a trapped curve as the intersection of two light cones with their vertices at the singular line. The curve becomes closed and smooth by the identification.

Finding examples of trapped curves is now easy. Consider the intersection

of two light cones with vertices at the singularity, as in Fig. 4.3. Light rays emanating from such curves obviously converge, and since they coincide with flow lines of the identifying transformation they are closed to smooth curves by the identification. Such curves are therefore trapped. These are not the only trapped curves in this spacetime, since we can take one of them and by wiggling it a bit obtain a new trapped curve. The light rays do not, as in this example, have to converge to a point.

The intersection of a light cone with its vertex at the singularity and the event horizon forms a marginally trapped curve. Remember that the event horizon in stereographic coordinates looks like a light cone with its vertex at the last point on $\mathcal{J}$, but we refer to it as a null plane, since lightlike geodesics on it have zero convergence. Unlike a trapped curve, a marginally trapped curve can not just as easily be wiggled in order to obtain a new marginally trapped curve; one must see to that it stays on the event horizon. The explicit expression of the marginally trapped curves we found is given by

$$\begin{cases} x = \pm(1-k) \\ v^2 - y^2 = k^2 \end{cases}, \quad 0 < k \leq 1. \tag{4.5}$$

Since these lie on the event horizon, the event horizon is in this case referred to as a *marginally trapped tube*. A marginally trapped tube is a surface foliated by marginally trapped curves. We see that in this case the foliation is not unique, since we can wiggle the marginally trapped curves we found in order to get a different foliation. The interior of the event horizon is filled with trapped curves, while there are none outside of it. The importance of the marginally trapped tube is that it separates the region containing trapped curves from the region free of them. For that reason, from now on we will mainly focus on the *marginally* trapped curves.

A spacelike surface in this spacetime will typically not contain one of the marginally trapped curves we found. This is not very practical in a computer simulation in which a family of spacelike surfaces describes the evolution of the spacetime. Unless these surfaces are chosen in a rather special way, no marginally trapped curves will be found. However, as long as one of these surfaces is smooth, it will always contain a closed curve on the event horizon. Light rays on the event horizon emanating from this curve have zero convergence. Such a curve, with no restriction on what happens with the light rays in the other direction, is said to be marginally *outer* trapped. With the same logic, a curve such that only one family of light rays converges, is said

to be *outer trapped*, with no restriction on the other family of light rays. Since a marginally outer trapped curve lies on the event horizon, it separates the region containing trapped curves from the region not containing trapped curves on the surface.

There is a theorem that says that a region of a spacelike surface bounded by an outer trapped curve in one direction and by an outer untrapped curve in the other direction must contain a marginally outer trapped curve [10]. In our spacetime this is almost obvious from the picture we have, as discussed in the previous paragraph. Note that the theorem would not be true if the word *outer* was omitted. For this reason, much of the literature [4, 10] discusses outer trapped surfaces.

To have the full picture though, we need to know if there are any other marginally outer trapped curves in our spacetime, apart from those we have already found on the event horizon. *Raychaudhuri's equation* [11] for a congruence of lightlike geodesics in 2+1 dimensions becomes

$$\dot{\theta} = -\theta^2 - R_{ab}k^a k^b, \tag{4.6}$$

where θ is the expansion of the congruence of geodesics, R_{ab} is the Ricci tensor and k^a is the tangent vector of a given geodesic. Since we have that $R_{ab} = \lambda g_{ab}$ and $k^2 = 0$ for a lightlike geodesic Eq. (4.6) becomes

$$\dot{\theta} = -\theta^2. \tag{4.7}$$

This shows that a congruence of lightlike geodesics that have zero expansion at one point, must continue to have zero expansion. Hence we conclude that marginally (outer) trapped curves must lie on a null plane. It should perhaps be remarked that this does not hold in 3+1 dimensions, since Raychaudhuri's equation then will contain extra terms. But it holds in our spacetime, so let us consider an arbitrary null plane in it. It is a light cone with its vertex at a point (x_0, y_0, v_0) on $\mathcal{J}$ and is described by

$$(x - x_0)^2 + (y - y_0)^2 = (v - v_0)^2, \quad x_0^2 + y_0^2 - v_0^2 = 1. \tag{4.8}$$

Suppose that a point (x, y, v) in this null plane also lies in one of the identification surfaces, i.e.

$$y = v \tanh \mu. \tag{4.9}$$

This point is identified with the point $(x', y', v') = (x, -y, v)$, which does not lie in the same null plane unless $y_0 = 0$. This shows that a null plane

with $y_0 \neq 0$ does not contain any closed curves. In the case with $y_0 = 0$ the question now is if there is a curve in the null plane connecting the two points (x, y, v) and (x', y', v') such that it is closed to a smooth curve by the identification. If so, the tangent vector of this curve at the point (x, y, v) is still tangent to the null plane at the point (x', y', v') after it is transformed by the identification. A tangent vector $\boldsymbol{t}$ in the null plane given by Eq. (4.8) (with $y_0 = 0$) at the point (x, y, v) is of the form

$$\boldsymbol{t} = \begin{pmatrix} t^x \\ t^y \\ t^v \end{pmatrix}, \quad (x - x_0)t^x + yt^y - (v - v_0)t^v = 0. \tag{4.10}$$

This is transformed into the vector

$$\boldsymbol{t}' = \begin{pmatrix} t'^x \\ t'^y \\ t'^v \end{pmatrix} = \begin{pmatrix} t^x \\ t^y \cosh 2\mu - t^v \sinh 2\mu \\ t^v \cosh 2\mu - t^y \sinh 2\mu \end{pmatrix}. \tag{4.11}$$

The vector $\boldsymbol{t}'$ is tangent to the null plane at the point (x', y', v') if

$$(x' - x_0)t'^x + y't'^y - (v' - v_0)t'^v = 0. \tag{4.12}$$

Using Eqs. (4.9) and (4.10) this simplifies to

$$v_0(t'^v - t^v) = 0. \tag{4.13}$$

This equation is satisfied either if $v_0 = 0$ (the considered null plane is then the event horizon) or if $t'^v = t^v$. In the latter case the tangent vectors, which are actually one and the same vector, lie in the identification planes. A curve with this tangent vector must stay in the same plane, heading towards $\mathcal{J}$. This is not the closed curve we were looking for. We have thus shown that all marginally (outer) trapped curves in this spacetime lie on the event horizon.

Chapter 5

How trapped curves jump

We are now ready to let a particle fall into the black hole of section 4. This is easily done by taking the point particle of section 3.3 and placing it in the BTZ spacetime. The point of this construction is that we will see how the trapped region suddenly jumps outwards.

The holonomy of the particle is $\boldsymbol{g}_1$, given by Eq. (3.10), and the holonomy of the singularity of the black hole is $\boldsymbol{g}_2$, given by Eq. (4.1). When combining these two we find a new holonomy $\boldsymbol{g}_1\boldsymbol{g}_2$. If we choose the constants a and μ such that $|\mathrm{Tr}\boldsymbol{g}_1\boldsymbol{g}_2| > 2$, the transformation $\boldsymbol{g} \to (\boldsymbol{g}_1\boldsymbol{g}_2)\boldsymbol{g}(\boldsymbol{g}_1\boldsymbol{g}_2)^{-1}$ has a spacelike line of fixed points. A new singularity has appeared. We can also see how this happens using a graphical approach (see Fig. 5.1). Considering the evolution on the Poincaré disk we see how the identification surfaces of the particle eventually begin to intersect the identification surfaces of the original black hole as the particle approaches the origin. These points of intersection are fixed points under the combined transformation $\boldsymbol{g}_1\boldsymbol{g}_2$, and they make up the new singularity. Using Eqs. (3.13) and (4.2), and switching to stereographic coordinates, we find that the last point on $\mathcal{J}$ is

$$(x_0, y_0, v_0) = A\,(a + \tanh\mu, \pm\, a\tanh\mu, a), \tag{5.1}$$

with

$$A = -\left(\frac{\coth\mu}{2a + (1+a^2)\tanh\mu}\right)^{1/2}. \tag{5.2}$$

This seems to be two distinct points, but we need to keep in mind that they are identified with each other, and therefore Eq. (5.1) describes just one single point. The singularity forms a line from this point to the origin,

and replaces the role of what used to be a singularity along the negative x-axis. But in this construction the positive x-axis is still a singular line. As before there are two last points on $\mathcal{J}$; one given by Eq. (5.1) and one at $(x, y, v) = (1, 0, 0)$. The new singularity comes with an event horizon consisting of the two light cones with vertices at these points. The event horizon will have a kink, it will not be smooth, before the particle crosses it. We need not worry about this, but note that it therefore contains no marginally trapped curves until the particle has passed. This kink, seen in Fig. 5.1(a), nicely illustrates the *teleological* nature of the event horizon. It has acquired a kink not because of something that has happened in the past, but because of something that will happen in the future.

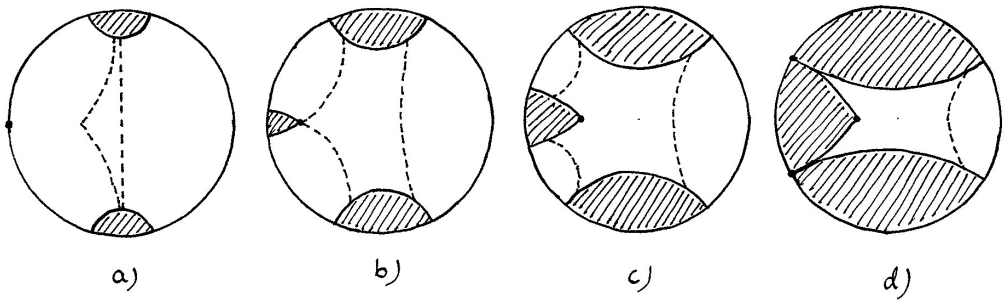

Figure 5.1: A sequence of Poincaré disks shows what happens when the particle falls into the black hole. (a) The particle comes in from infinity at $t = -\pi/2$. At this point the event horizon has a kink and does not contain any marginally trapped curves. (b) At a later time the particle meets the event horizon. (c) After the particle has passed the event horizon, the horizon is turned into a smooth surface by the identification and now contains marginally trapped curves. (d) When the identification surfaces of the particle and the original black hole begin to intersect a new set of fixed points appear.

The path of the particle lies on a light cone with its vertex at the origin. This light cone actually splits into two by the identification, but consider the one where the x-coordinate is negative, since this is the surface on which the particle travels. In the quotient space it really is a smooth cone, and it divides the spacetime into two parts with different properties. Inside the light cone everything looks just like the BTZ spacetime. If restricted to this region there is no way to distinguish it from the BTZ black hole, since the holonomy $\boldsymbol{g}_2$ is the same. But what used to be the event horizon at

$(x+1)^2 + y^2 = v^2$ is no longer the event horizon. We know this since we have a complete picture of the spacetime. But the trapped curves remain. Smooth curves on the old event horizon are still marginally outer trapped. Light rays emanating from these curves still behave as if they were heading towards the point $(x, y, v) = (-1, 0, 0)$. They will not reach this point, since we know that they will hit the singularity before they get there, but the only thing that matters is that they have zero convergence. The old event horizon is now referred to as an *isolated horizon* [12]. After the particle has crossed it, it will no longer be smooth and therefore contain no marginally (outer) trapped curves.

Outside the light cone on which the particle travels things look quite different. The holonomy is $\boldsymbol{g}_1\boldsymbol{g}_2$. After the particle has passed the event horizon, which then will become smooth, marginally trapped curves will suddenly appear in this region. As before they consist of intersections of light cones with vertices at the singular line and the event horizon.

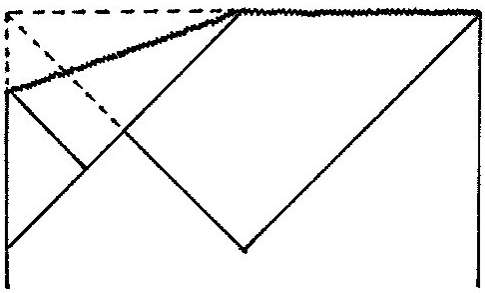

Figure 5.2: Conformal diagram of the black hole spacetime obtained when a particle falls into the BTZ black hole. The dotted lines show what used to be the singularity and the event horizon when the particle was not present. The light cone on which the particle travels is represented by the lightlike line ending at the origin. Inside of this light cone the marginally trapped curves lie on the isolated horizon and outside of the light cone they lie on the event horizon. This shows how the trapped region "jumps" outwards.

It is clear that it can not be determined if a curve is trapped by looking at it locally. For example, a curve on the event horizon which locally seems trapped may not be genuinely trapped. It must be closed, and whether it is closed or not is determined in a different part of space. What used to be the event horizon in the BTZ spacetime contains marginally trapped curves

before it is hit by the particle. After it is hit it no longer contains closed smooth curves, hence no marginally trapped curves. Instead other closed curves that are marginally trapped appear in a different region of space; the trapped curves "jump". The whole picture is quite nicely illustrated in Fig. 5.2. It shows a conformal diagram [2] of this spacetime in which we clearly see how the trapped region jumps outwards due to the particle. The marginally trapped tube now consists of two parts. Inside the light cone on which the particle travels it consists of the isolated horizon, and outside the light cone it consists of the event horizon. The transition of the marginally trapped curves from the isolated horizon to the event horizon shows how they "jump". This is in fact a reasonable illustration of the problem with a particle hitting a trapped surface, mentioned in the introduction (Fig. 1.2).

Chapter 6

Open ends

During the work of this thesis, new ideas and problems have naturally arisen. There are at least two questions left unanswered, and a natural way to end this thesis is by listing these.

- In the previous chapter we saw that the marginally trapped tube split into two parts. One part being the isolated horizon and the other part forming part of the event horizon. These could not be connected in the model we had, since there was a singularity in the form of a point particle in between. In a more complicated model, one could consider a small mass distribution instead of a point particle [5]. The hope of doing this would be to find a spacelike component of the marginally trapped tube, a so-called *dynamical horizon* [12], connecting the isolated horizon with the event horizon.

- An interesting complication encountered during the work of this thesis is the *three-body problem*. How a black hole can be created by colliding two particles was shown by Matschull [9]. It was later shown by Holst and Matschull [13] how a spinning black hole can be created by letting two particles pass each other without colliding. It turns out that when doing something similar with three particles involved, the spin of the black hole behaves in a seemingly counterintuitive way. This is something that could be worth investigating further.

Bibliography

[1] Bañados M, Teitelboim C and Zanelli J 1992 *Phys. Rev. Lett.* **69** 1849

[2] Penrose R 1968 "Structure of Space-Time" in *Battelle Rencontres: 1967 lectures in mathematics and physics*, ed. C M DeWitt and J A Wheeler (W. A. Benjamin, New York)

[3] Jaramillo J L, Ansorg M and Vasset N 2009 *AIP Conf. Proc.* **1122** 308

[4] Andersson L, Mars M and Simon W 2005 *Phys. Rev. Lett.* **95** 111102

[5] Giddings S, Abbott J and Kuchař K 1984 *General Relativity and Gravitation* **16** 8

[6] Holst S 2000 *Horizons and Time Machines - Global Structures in Locally Trivial Spacetimes*, PhD thesis, Stockholm University

[7] Schutz B 2009 *A First Course in General Relativity* (Cambridge University Press, Cambridge)

[8] Ellis G F R and Hawking S W 1973 *The Large Scale Structure of Space-Time* (Cambridge University Press, Cambridge)

[9] Matschull H-J 1999 *Class. Quant. Grav.* **16** 1069

[10] Andersson L and Metzger J 2009 *Commun. Math. Phys.* **290** 941

[11] Wald R M 1984 *General Relativity* (University of Chicago Press, Chicago)

[12] Ashtekar A and Krishnan B 2004 *Living Rev. Relativity* **7** 10. URL (cited on 3 June 2011): http://www.livingreviews.org/lrr-2004-10

[13] Holst S and Matschull H-J 1999 *Class. Quant. Grav.* **16** 3095